Highly Sensitive Determination of the Polaron-Induced Optical Absorption of Organic Charge-Transport Materials

T. Rabe,[1] P. Görrn,[1] M. Lehnhardt,[2] M. Tilgner,[1] T. Riedl,[1,*] and W. Kowalsky[1]

[1]*Institut für Hochfrequenztechnik, Technische Universität Braunschweig, Schleinitzstrasse 22, 38106 Braunschweig, Germany*

[2]*Physikalisch-Technische Bundesanstalt, Bundesallee 100, 38116 Braunschweig, Germany*

(Received 27 May 2008; published 30 March 2009)

We examine polaron-induced absorption in organic transport materials using a highly sensitive measurement technique. A hole only device is embedded into a low-loss TE_2 waveguide structure, and the current induced change of the waveguide absorption is measured. The exemplary study of 2, 2′, 7, 7′-tetrakis(*N*, *N*-diphenylamine)-9, 9′-spiro-bifluorene (S-TAD) reveals a very low polaron absorption cross section of $\sigma_p \leq 2.6 \times 10^{-18}$ cm^2 for 560 nm $\leq \lambda \leq$ 660 nm. The accuracy of this data is unsurpassed by other techniques used for the unambiguous study of polaronic species in organic thin films.

DOI: 10.1103/PhysRevLett.102.137401 PACS numbers: 78.66.Qn, 42.70.Jk, 78.45.+h

Polaron related absorption in organic materials is of interest not only from a fundamental point of view but has also significant implications for various device applications. Especially, for electrically operated organic laser structures, precise information about charge induced absorption is essential [1,2]. There have been some reports dealing with the spectroscopy of charged states in both polymers and small molecules. A plethora of these study polaron absorption via photoinduced absorption techniques, where the generation of polaronic species relies on the dissociation of generated excitons [3,4]. The mechanism of charge generation in these experiments only allows for a rough estimate of the actual carrier density. A unique assignment of the origin for the observed change in absorption to a particular carrier species is not always straightforward. An alternative approach is based on electrochemical experiments, where both solutions and solid films have been studied in redox cycles in an electrolyte. However, these studies suffer from irreversibilities and hysteresis [5]. In the case where chemical doping is used to create charged molecules, the absorption due to the counterion is superimposed. Furthermore, Walzer *et al.* report on incomplete charge transfers, making a determination of the exact density of generated charge carriers difficult [6].

An unambiguous way to spectroscopically determine the charge induced absorption in organic thin films is the direct, controlled injection and extraction of charges (holes or electrons) through contacting electrodes [7]. Owing to the poor charge-transport capabilities in most organic amorphous films, the maximum film thickness to reach reasonable current densities in unipolar transport devices is limited. Therefore, the most straight forward spectroscopical study of the resulting polaron absorption in transmission geometry lacks accuracy due to limited signal/noise ratio [7].

In this Letter, we will present a highly sensitive technique to quantitatively determine the polaron-induced absorption. In unipolar devices, we exemplarily study the hole-transport material S-TAD. Based on low-loss waveguide structures with charge injection contacts [8,9], we are very sensitive to any current or carrier-related change in absorption. Owing to a length for the interaction of the optical mode with the polaronic species in the organic layer of the order of mm's rather than hundreds of nm's as in conventional transmission geometry, the sensitivity for the detection of carrier induced absorption is increased by 2–3 orders of magnitude compared to those reported previously, e.g., by Redecker *et al.* [7].

By comparing the spectral signature to that obtained in reference experiments on chemically doped S-TAD films, we unambiguously identify S-TAD cations as the origin for the current induced absorption. In the absorption maximum at $\lambda \approx 500$ nm, a cross section of $\sigma_p = 3.8 \times 10^{-17}$ cm^2 is found. Importantly, in the spectral region between 560 nm $\leq \lambda \leq$ 660 nm, the cross section for polaron-induced absorption is below $\sigma_p = 2.6 \times 10^{-18}$ cm^2.

All organic films have been thermally evaporated at a pressure of about 1×10^{-8} mbar. Al_2O_3 buffer layers were deposited by atomic layer deposition at 250 °C. Indium Tin Oxide (ITO) electrodes have been deposited by rf magnetron sputtering at room temperature. The core of the experimental setup is the use of a low-loss waveguide structure based on the propagation of the TE_2 mode [8]. Waveguide absorption is minimized for the TE_2 mode by positioning the lossy ITO electrodes in the nodes of the mode [Fig. 1(a)]. As optical buffer on top of the structure, a layer of Tris-(8-hydroxy-quinoline)aluminum (Alq_3) was used. To tune the wavelength range of the measurement, three samples were prepared, where the thickness of the Alq_3 buffer was varied (A: 240 nm, B: 280 nm, C: 320 nm). Furthermore, this layer serves as the light source for the waveguide characterization [8]. Therefore, the overall spectral limit is given by the photoluminescence of Alq_3 and its increasing absorption below 500 nm. The electrical part of the structure consists of a 15 nm thick ITO electrode

(substrate side) with an injection layer of 10 nm TCTA:WO_3 (5 vol%) to enhance Ohmic hole injection into the 270 nm thick S-TAD layer [10]. The upper ITO electrode (40 nm) was sputtered directly on the S-TAD layer. Rectangular voltage pulses (pulse width: 2 μs, rep. rate: 2 kHz) were synchronized with the optical pulses. The J-V characteristic shows a rectifying behavior with the charge injection via the bottom electrode being a factor of $\geq 10^2$ larger than that via the top electrode under reverse bias (see inset of Fig. 2).

The mode simulation is based on a transfer matrix algorithm [11] taking the dispersion of the refractive indices into account. TM modes are excluded from the measurement using a polarization filter. The waveguide absorption has been determined by the variable stripe length (VSL) method as described previously [8]. For the electro-optic experiments, only a small segment ($100 \times 200\ \mu m^2$) a distance L away from the sample edge was excited optically and the edge emission was detected [see Fig. 1(b)]. The waveguide length L was between 1.7 and 2.8 mm. The width of the waveguide was 100 μm. The reference signal was taken under the same optical conditions without charge injection. As we are studying a hole only structure, radical cations are the prevalent species. During the measurements, the samples were mounted in a Nitrogen purged sample chamber to avoid degradation. The chemically doped solution was prepared by adding 5 ± 0.5 mol% of F4-TCNQ to S-TAD dissolved in CH_2Cl_2. The absorption measurements were performed in transmission geometry. The doped films were prepared by co-evaporation of S-TAD and F4-TCNQ (5 ± 2 mol%). Losses were measured in waveguide geometry as described previously [12].

A characteristic feature of the TE_2 approach is the limited spectral region where the optical losses of the TE_2 mode are extremely low. Nevertheless, for our samples, spectral windows on the order of 80 nm were obtained. Furthermore, by sequentially increasing the upper buffer layer thickness, the structure is easily tunable to longer wavelengths. Figure 1(c) shows the spectrally resolved waveguide losses obtained by VSL measurements for samples A, B, and C. In addition, the simulated losses are superimposed. There is a favorable agreement between measurement and simulation. The difference in the waveguide losses of the TE_2 compared to the other modes is typically more than 1 order of magnitude. The three samples cover the spectral range between 500 and 660 nm with absorption minima of 14.0, 6.0, and 10.1 cm^{-1} for sample A, B, and C, respectively. Note that the entire stack was optimized for minimum losses of sample B.

The spatial overlap of the TE_2 mode with the S-TAD layer is $\Gamma(\lambda) \approx 15\%$ and remains virtually constant in the spectral region of the experiment. For the determination of the polaron absorption, the edge emission spectra with and without hole current are compared. The absorption of the charge carriers $\alpha_p(\lambda)$ can be calculated from the change of the spectra upon application of a current pulse as follows:

$$\alpha_p(\lambda) = \frac{\Delta\alpha_w(\lambda)}{\Gamma(\lambda)} = \frac{1}{\Gamma(\lambda)L} \ln\frac{I_{\mathrm{off}}(\lambda)}{I_{\mathrm{on}}(\lambda)}. \quad (1)$$

$I_{\mathrm{off}}(\lambda)$ and $I_{\mathrm{on}}(\lambda)$ are the edge emission spectra with and without hole current, L is the length of the waveguide, $\Gamma(\lambda)$ is the confinement factor of the mode in the S-TAD layer.

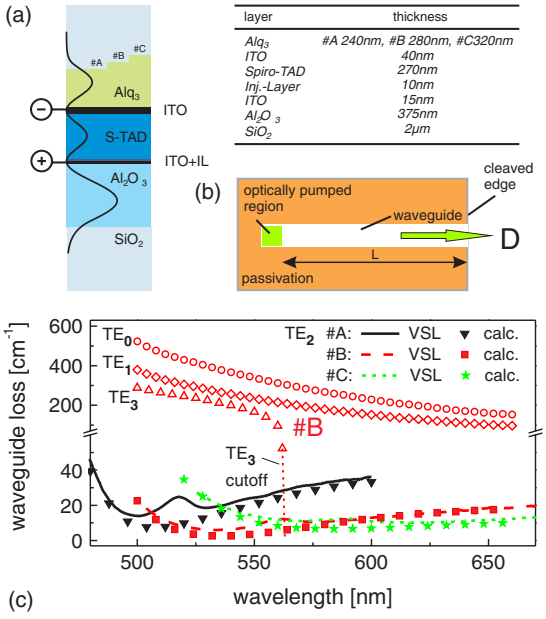

FIG. 1 (color online). (a) Cross section through the devices, TE_2 mode profile, and layer thicknesses (Table); (b) Principle of the excitation and detection geometry for the electro-optic experiment; (c) Fundamental waveguide losses of samples A–C: VSL results and calculation, as well as the numerical simulation of the losses for the TE_0-, TE_1-, and TE_3-modes of sample B.

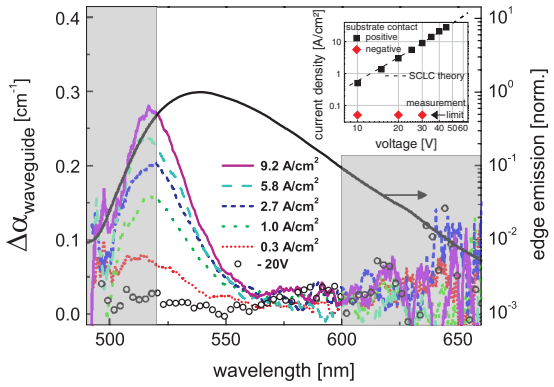

FIG. 2 (color online). Sample B: Current induced absorption spectra up to 9.2 A/cm^2, the window region is the selected spectral region (see text). Inset: Current density voltage characteristics in forward and reverse direction for the unipolar device structure. The dashed line indicates the calculated space charge limited current (SCLC) density. The field-dependent mobility has been taken from Ref. [16].

The changes of the waveguide absorption $\Delta\alpha_w(\lambda)$ in sample B are shown in Fig. 2. It is important to note that we do not see any absorption when the polarity of the electrical pulse is reversed (open circles). Thus, we can exclude that the signal we see is field-related rather than carrier-related. The spectra were taken for various hole current densities up to $J = 9.2$ A/cm^2. In the shaded region for $\lambda > 600$ nm, the signal/noise ratio decreases due to the decreasing edge intensity. Therefore, we use the results of sample C for $\lambda > 600$ nm. For $\lambda < 520$ nm, contributions from higher cutoff modes (e.g., TE_4) affect the measurements. Hence, in this spectral region, the results of sample B must be excluded from the interpretation of the polaron absorption, and the results of the adjoining sample A are used.

Figure 3(a) shows the combined polaron absorption resulting from samples A, B, and C at 9.2 A/cm^2. An absorption maximum is observed at $\lambda \approx 500$ nm with a material absorption due to radical cations of 2.9 cm^{-1}. For $\lambda > 560$ nm, the polaron absorption drops to the noise level. The detection limit for these absorption measurements is determined by the maximum length of the waveguide and the temporal fluctuations of the measurement components. In our experiments, an edge intensity variation of $\approx 1\%$ due to polaron absorption could be well resolved. This leads to a minimum detectable change in waveguide absorption of $\Delta\alpha_w \approx 0.03$ cm^{-1}. This value corresponds well to the observed noise level of sample B and C. Hence, any absorption losses due to polarons in S-TAD between 560 and 660 nm must be lower than 0.2 cm^{-1} for current densities up to 9.2 A/cm^2.

In order to verify the spectral position of the measured polaron absorption, we studied the absorption spectra of chemically doped S-TAD. In Fig. 3(a), we clearly see that the spectra obtained for doped films and solutions are similar to the spectrum measured by direct charge injection. Note, the absorption seen for $\lambda > 560$ nm in the F4-TCNQ doped case is attributed to the absorption due to the F4-TCNQ anion [13] which is absent in the current induced absorption spectra.

To relate the absorption to the density of injected charge carriers, a space charge limited current (SCLC) is considered [14]. The assumption of SCLC is supported by the favorable agreement between the measured and the calculated current density (see inset of Fig. 2). The current-voltage characteristics and the spatial distribution of the charge carrier density inside the S-TAD layer were calculated using the field-dependent mobility based on the disordered formalism suggested by Bässler, which has been verified for a variety of amorphous molecular glasses [15,16]. In the case of SCLC, there is a charge accumulation close to the injecting electrode [see Fig. 3(b)]. Concerning the TE_2 concept, the mode intensity has a very small spatial overlap with this region. The simulated carrier distribution $p(x)$ was weighted with the simulated TE_2 mode intensity and the integral average was calculated to derive the effective polaron density, which causes the waveguide absorption. For example, at a current density of 10 A/cm^2, the effective polaron density is 7.6×10^{16} cm^{-3}. Figure 4 shows the polaron absorption of sample A at 500 nm versus the charge carrier density. Both characteristics show an excellent agreement in their functional behavior. As a result, the measured polaron absorption increases linearly with the average carrier density in the device. Thus, we are able to determine a cross section of $\sigma_p = 3.8 \times 10^{-17}$ cm^2 at 500 nm.

There is a reasonable agreement of our data and the cross section of 1×10^{-16} cm^2 (at ~480 nm) determined for radical cations of *N, N, N′, N′*-Tetraphenylbenzidine (TAD) molecules by Low and co-workers [17]. The spiro linkage of two identical molecules has been shown to retain their individual properties [18]. Thus, comparable polaron sprectra for TAD and S-TAD are expected. Unfortunately, there is no discussion of a spectral window where the polaron absorption in TAD would be small and thus favorable for, e.g., laser applications. In Tris-(dimethylamino-stilbene)-amine, Redecker *et al.* found a cross section for the absorption due to cations of

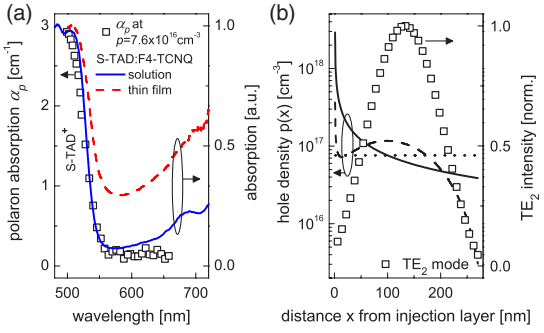

FIG. 3 (color online). (a) Radical cation absorption spectra obtained by direct current injection (open squares) compared to data obtained from absorption measurements on chemically doped S-TAD in solution and thin film; (b) Hole density (solid line), weighted hole density (dashed line) and the resulting average hole density (dotted line) for a current density of 10 A/cm^2.

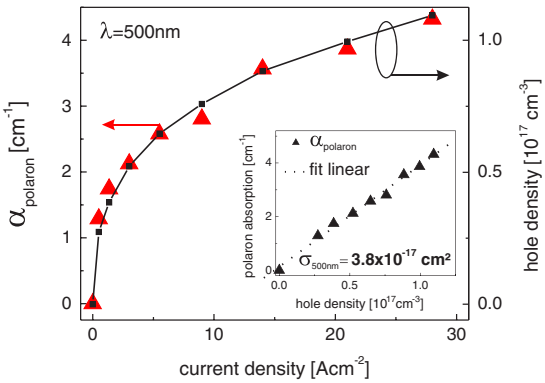

FIG. 4 (color online). Sample A: Polaron absorption and charge carrier density versus current density at $\lambda = 500$ nm. The inset shows the derived polaron absorption versus hole density.

8.3×10^{-17} cm^2 at 600 nm and also a drop towards longer wavelengths [7]. However, probably due to the limited dynamics of their measurement, the minimum cross section of approx. 3.4×10^{-17} cm^2 at 775 nm is still large compared to our data (for $\lambda > 560$ nm). Kurata *et al.* have studied the absorption due to radical cations in α-sexithiophene [19]. They observed a spectral maximum at 800 nm with a cross section of 4.6×10^{-17} cm^2 by field-effect induced charges. On the other hand, in the same material and in the same paper, a value of 3.4×10^{-16} cm^2 is determined in chemically doped solutions. This again demonstrates the need for an unambiguous determination of the polaron related absorption.

From an application point of view, the spectral range where the polaron absorption is below the noise level is extremely interesting. Here, we can give an estimation for the upper boundary of the cross section of $\sigma_p = 2.6 \times 10^{-18}$ cm^2 for $\lambda > 560$ nm. Numerous authors have identified polaron-induced absorption as a premier obstacle on the way to an electrically driven organic laser [1,2,20]. Our finding now literally opens up a window (spectrally) where charges may be present without creating serious losses. With a cross section for polaron absorption orders of magnitude lower than cross sections for stimulated emission, electrically operated organic lasers might ultimately become feasible [20]. The minimum absorption was found in the wavelength range between the two absorption features, which are characteristic for cationic polarons [21]. In TAD-like structures, the reported absorption peaks are located at 484 and 1384 nm [17,22]. These features are due to electronic transitions involving the formed singly occupied highest molecular orbital (SOMO), which emerges upon charging. The large separation of the peaks is a consequence of the small energy shift of the states, determined by polarization and reorganization effects during ionization. Small reorganization energies have been reported for tri-phenylamines, and are responsible for the high mobility in these compounds [23]. Hence, the large spectral peak separation leads to a spectrally broad absorption minimum of the charged tri-phenylamine molecules. Quantum chemical calculations of a charged TAD molecule show that the SOMO orbital is delocalized over the entire molecule, whereas the LUMO is localized on the biphenyl moiety [24]. This spatial separation may be an indication for a low transition probability and a relatively small oscillator strength.

To estimate the impact of the polaron absorption for organic lasers, high injection levels must be considered. At a current density of 1000 A/cm^2, the effective charge carrier density is about 2.9×10^{17} cm^{-3}. Hence, at 500 nm, the material absorption induced by polarons would be 11.0 cm^{-1}. However, most importantly, within the spectral range from 560 to 660 nm, the polaron absorption is lower than 0.76 cm^{-1}, which results in additional waveguide losses well below typically intrinsic waveguide losses on the order of 1 cm^{-1}. Our exemplary study of the representative S-TAD is expected to provide some general picture for the polaron related absorption in other members of this class like *N, N′*-diphenyl-*N, N′*-Bis(3-methylphenyl)-(1, 1′-biphenyl)-4, 4′-diamine (TPD), *N, N, N′, N′*-Tetrakis(4-methylphenyl)benzidine (TTB) and 4,4', 4''-tris(diphenylamino)-triphenylamine (TDATA), etc.

In summary, we have investigated the polaron-induced absorption of organic transport layers. In an exemplary study at the hole-transport material S-TAD, we measured a maximum polaron absorption cross section of $\sigma_p = 3.8 \times 10^{-17}$ cm^2 at $\lambda \approx 500$ nm. For 560 nm $\leq \lambda \leq$ 660 nm, the absorption was below the detection limit of $\alpha_p = 0.2$ cm^{-1} resulting in an upper limit of the cross section of $\sigma_p = 2.6 \times 10^{-18}$ cm^2. Because of the low polaron absorption cross section, the results of this study have particular relevance for the design of organic injection lasers. Furthermore, the exact knowledge of the charge carrier absorption is an important information to include polaron related quenching effects in the modeling of organic light emitting diodes.

We gratefully acknowledge financial support by the German Federal Ministry for Education and Research BMBF (FKZ 13N8166A).

*t.riedl@tu-bs.de

[1] M. A. Baldo, R. J. Holmes, and S. R. Forrest, Phys. Rev. B **66**, 035321 (2002).
[2] C. Gärtner *et al.*, J. Appl. Phys. **101**, 023107 (2007).
[3] P. A. Lane, X. Wei, and Z. V. Vardeny, Phys. Rev. Lett. **77**, 1544 (1996).
[4] M. A. Stevens *et al.*, Phys. Rev. B **63**, 165213 (2001).
[5] S. Janietz *et al.*, Appl. Phys. Lett. **73**, 2453 (1998).
[6] K. Walzer *et al.*, Chem. Rev. **107**, 1233 (2007).
[7] M. Redecker and H. Bässler, Appl. Phys. Lett. **69**, 70 (1996).
[8] P. Görrn *et al.*, Appl. Phys. Lett. **91**, 041113 (2007).
[9] P. Görrn *et al.*, Appl. Phys. Lett. **89**, 161113 (2006).
[10] J. Meyer *et al.*, J. Mater. Chem. **19**, 702 (2009).
[11] R. E. Smith, S. N. Houde-Walter, and G. W. Forbes, IEEE J. Quantum Electron. **28**, 1520 (1992).
[12] T. Rabe *et al.*, Appl. Phys. Lett. **90**, 151103 (2007).
[13] X. Zhou *et al.*, Adv. Funct. Mater. **11**, 310 (2001).
[14] M. A. Lampert and P. Mark, *Current Injection in Solids* (Academic Press, New York, 1970).
[15] Y. Shirota and H. Kageyama, Chem. Rev. **107**, 953 (2007).
[16] U. Bach *et al.*, Adv. Mater. **12**, 1060 (2000).
[17] P. J. Low *et al.*, J. Mater. Chem. **15**, 2304 (2005).
[18] T. P. I. Saragi *et al.*, Chem. Rev. **107**, 1011 (2007).
[19] T. Kurata *et al.*, Thin Solid Films **331**, 55 (1998).
[20] N. Tessler, Adv. Mater. **11**, 363 (1999).
[21] E. Zojer *et al.*, Phys. Rev. B **59**, 7957 (1999).
[22] K. Yuan Chiu *et al.*, J. Electroanal. Chem. **575**, 95 (2005).
[23] M. Malagoli and J. L. Brédas, Chem. Phys. Lett. **327**, 13 (2000).
[24] P. J. Low *et al.*, Chem. Eur. J. **10**, 83 (2004).